THE JOURNAL OF PHYSICAL CHEMISTRY B

Article

pubs.acs.org/JPCB

Redox Potentials of Protein Disulfide Bonds from Free-Energy Calculations

Wenjin Li,[†,‡,§] Ilona B. Baldus,[†,§] and Frauke Gräter*[,†]

[†]Heidelberg Institute for Theoretical Studies, Schloss-Wolfsbrunnenweg 35, 69118 Heidelberg, Germany

Supporting Information

ABSTRACT: Thiol/disulfide exchange in proteins is a vital process in all organisms. To ensure specificity, the involved thermodynamics and kinetics are believed to be tailored by the structure and dynamics of the protein hosting the thiol/disulfide pair. We here aim at predicting the thermodynamics of thiol/disulfide pairs in proteins. We devise a free-energy calculation scheme, which makes use of the Crooks Gaussian intersection method to estimate the redox potential of thiol/disulfide pairs in 12 proteins belonging to the thioredoxin superfamily, namely, thioredoxins, glutaredoxins, and thiol−disulfide oxidoreductases in disulfide bond formation systems. We obtained a satisfying correlation of computed with experimental redox potentials (varying by 160 mV), with a residual error of ∼40 mV (8 kJ/mol), which drastically reduces when considering a less diverse set of only thioredoxins. Our simple and transferrable approach provides a route toward estimating redox potentials of any disulfide-containing protein given that its (reduced or oxidized) structure is known and thereby represents a step toward a rational design of redox proteins.

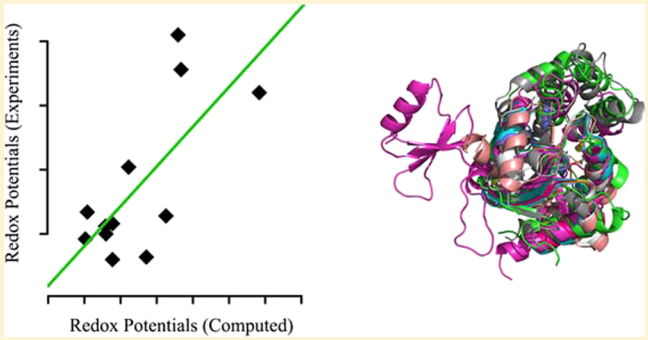

INTRODUCTION

Redox reactions play a key role in biology. They regulate processes as diverse as energy metabolism, respiration, photosynthesis, gene expression, signal transduction, and protein folding.[1−3] The mitochondrial respiratory chain, for example, is well understood and has revealed that redox events are tightly controlled by proteins or enzymes.[4] Cysteines are the residues in a protein most commonly involved in redox reactions, and thiol/disulfide exchange is the most common reaction that cysteines undergo in living systems. Enzymes such as thioredoxins (Trx), glutaredoxins (Grx), and thiol−disulfide oxidoreductases in disulfide bond formation systems (Dsb) play fundamental roles in such redox reactions.[5,6] Trx and Grx are small enzymes involved in redox signaling.[7,8] Dsb is responsible for the introduction and isomerization of disulfide bonds in proteins.[6] They all contain a *CXXC*-motif that was shown to be essential for their oxidoreductase activities,[9] and they catalyze not only the oxidation of thiols to disulfides and the backward reaction but also disulfide isomerization. Mutations of the C-terminal amino acid of the *XX* dipeptide in Trx have shown that this sequence has a strong impact on the redox potential.[9,10] Given their importance, it is desirable to establish techniques that offer easy access to redox potentials and the factors that influence them.[11]

Determining redox potentials of proteins experimentally is elaborate. In principle, redox potentials can be calculated from the concentration of the reducing agent during titration.[12] However, though redox potentials can be measured experimentally quite precisely, measured redox potentials are known to vary depending on the (proteineous) redox partner and experimental conditions. Also, tuning a redox potential by protein mutagenesis is resource intensive, as the effects of a single mutant on a disulfide bond's stability depend on several factors. More precisely, the structure of the protein, the pK_a value of the disulfide, the strain on the bond, and the protein's electrostatic environment have a large impact on the redox potential.[9] Thus, having a fast and simple way to calculate redox potentials of thiol/disulfide pairs from molecular dynamics (MD) simulations would be desirable.

Several methods have been introduced over the past decades that provide ways to calculate redox potentials. The spectrum ranges from density function theory to calculate not only the redox potential but also the electronic structure of metal ions[13] to pure molecular mechanics (MM) approaches.[14] Calculations of individual metal ions or metal complexes typically use pure quantum mechanical (QM) descriptions.[13,15] For taking the effect of a protein surrounding into account, a hybrid quantum mechanical/molecular mechanical (QM/MM) approach has been proven useful,[16−19] but also mere classical descriptions have been demonstrated to successfully predict redox properties of enzymes which contain a reactive metal center that changes its redox state.[14,20,21]

We here propose a method to calculate redox potentials of protein disulfide bonds using MM and will discuss its strengths

Received: February 1, 2015
Revised: April 8, 2015
Published: April 9, 2015

DOI: 10.1021/acs.jpcb.5b01051
J. Phys. Chem. B 2015, 119, 5386−5391

and bottlenecks. Thiol/disulfide exchange is more challenging than the widely studied cases of metal ion redox chemistry. Redox reactions involving metal ions primarily require a change in the ion parameters (charge and van der Waals parameters), while a disulfide reduction involves bonded interactions to turn into nonbonded ones and hydrogen atoms to appear. We chose several proteins and their mutants in the thioredoxin superfamily, which all contain a *CXXC* motif but which span a broad range of redox potentials, to test the proposed method. Our method allows the prediction of redox potentials of disulfide bonds in various proteins within an accuracy of 40 mV (8 kJ/mol), that is, it is able to distinguish between larger variations in redox potentials.

COMPUTATIONAL METHODS

According to Nernst's equation, the redox potential (E^0) is related to the free-energy difference (ΔG) between the reactant and product states in a redox reaction:

$$E^0 = -\Delta G/nF \tag{1}$$

where n is the number of electrons transferred and F is the Faraday constant. Thus, the calculation of a redox potential comes down to the calculation of the free-energy change, for which various approaches have been developed.

Crooks Gaussian Intersection Method. Here, we use the Crooks Gaussian intersection (CGI) method to calculate free-energy differences between reduced and oxidized states in redox reactions. As the method has already been described in detail in the literature,[22] we here provide only a simplified description.

For a transition from the reduced to the oxidized state, each state along the transition is defined by the Hamiltonian H_λ, which is a linear combination of the Hamiltonians of the reduced (H_0) and the oxidized state (H_1):

$$H_\lambda = (1 - \lambda)H_0 + \lambda H_1 \tag{2}$$

Here, λ is the coupling parameter, which switches from 0 to 1 gradually and forces the transition from the reduced state to the oxidized state. For an arbitrary transition time τ, the work over the transition is given by

$$W(\tau) = \int_0^1 \frac{\delta H_\lambda}{\delta \lambda} \mathrm{d}\lambda \tag{3}$$

For an infinitely slow transition (i.e., $\tau \to \infty$), eq 3 gives the exact free-energy difference between the reduced state and the oxidized one (ΔG). For any finite τ, the transition is a nonequilibrium process, and a work distribution $P(W)$ will be obtained. Both forward and backward transitions can be induced by transforming λ from 0 → 1 or 1 → 0, respectively. According to Crooks' fluctuation theorem (CFT),[23,24] the work distributions for forward ($P_f(W)$) and backward ($P_b(-W)$) transitions obey

$$\frac{P_f(W)}{P_b(-W)} = \exp[\beta(W - \Delta G)] \tag{4}$$

It relates the free-energy difference ΔG to the work distributions in the forward and backward ensemble of nonequilibrium transitions.

According to eq 4, $W = \Delta G$ when $P_f(W) = P_b(-W)$. Thus, the intersection point of the forward and backward work distributions gives the value of ΔG. It has been shown that the work distribution $P(W)$ can be approximated by a Gaussian function[22]

$$P_{f,b}(W) \sim \frac{1}{\sigma_{f,b}\sqrt{2\pi}} \exp\left[-\frac{(W - W_{f,b})^2}{2\sigma_{f,b}^2}\right] \tag{5}$$

where $W_{f,b}$ and $\sigma_{f,b}$ are the mean and standard deviation of the forward and backward work, respectively. By assuming the work distribution to be Gaussian, the solution of equation $P_f(W) = P_b(-W)$ or the free-energy difference ΔG is

$$\Delta G = \frac{\frac{W_f}{\sigma_f^2} - \frac{-W_b}{\sigma_b^2} \pm \sqrt{\frac{1}{\sigma_f^2\sigma_b^2}(W_f + W_b)^2 + 2\left(\frac{1}{\sigma_f^2} - \frac{1}{\sigma_b^2}\right)\ln\frac{\sigma_b}{\sigma_f}}}{\frac{1}{\sigma_f^2} - \frac{1}{\sigma_b^2}} \tag{6}$$

For work distributions with $\sigma_f \neq \sigma_b$, eq 6 results in two intersection points. Typically, if two results are obtained, one is close to the mean value of the two distributions, and the other one can be found in the tail region of the work distributions. In general, the intersection point closer to the mean is the appropriate estimate of ΔG.

Simulation Setup. All molecular dynamics (MD) simulations were carried out using the GROMACS-4.5.5 package.[25] The CHARMM27 force field was applied. Each protein studied here was solvated in a box of explicit water of TIP3P.[26] The box was large enough to allow at least a 1.2 nm distance in all directions. A salt concentration of 0.1 mol/L was chosen to mimic physiological conditions and to neutralize the system.

We used a time step of 2 fs and periodic boundary conditions for all simulations. First, the system was energy minimized using the steepest descent algorithm. Next, the water was equilibrated while the motion of the heavy atoms of the protein was restrained with a spring constant of 1000 kJ/(mol·nm^2) at 300 K for 100 ps. Then, we released the position restraints and performed the production simulation for 15 ns in the NpT ensemble. The temperature was controlled using velocity rescaling;[27] the time step for temperature coupling was chosen as 0.4 ps. Protein and solvent were separately coupled to the thermostat. The pressure was kept at 1 bar, using isotropic pressure coupling via the Parrinello−Rahman barostat and a coupling constant of 1.0 ps. The Lincs constraint[28] was used on all bonds containing a hydrogen atom. Nonbonded interactions were calculated within a cutoff of 1.0 nm. Electrostatic interactions beyond 1.0 nm were treated with particle-mesh Ewald (PME)[29] with a grid spacing of 0.12 nm. Nonbonded interactions were calculated with soft-core potentials.[30,31] The soft-core parameter α, which controls the height of the potential at zero distance, was set to 1.2.[32] The interaction radius σ was calculated from the Lennard-Jones (LJ) parameters, with $(C12/C6)^{1/6}$ for C12, C6 ≠ 0, otherwise σ = 0.3. The soft-core parameters were also taken into account explicitly for short-range interactions and beyond the nonbonded cutoff in the PME calculations as implemented in GROMACS.[33]

Hybrid Cysteine/Cystine Force Field. We used CGI to calculate the difference in free energy and thus the redox potential of proteins that undergo reduction of their disulfide bonds, as shown in Figure 1. In CGI, the parameter λ switches the system in an alchemical transformation from the oxidized to the reduced state. Thereby, the disulfide bond needs to be

DOI: 10.1021/acs.jpcb.5b01051
J. Phys. Chem. B 2015, 119, 5386−5391

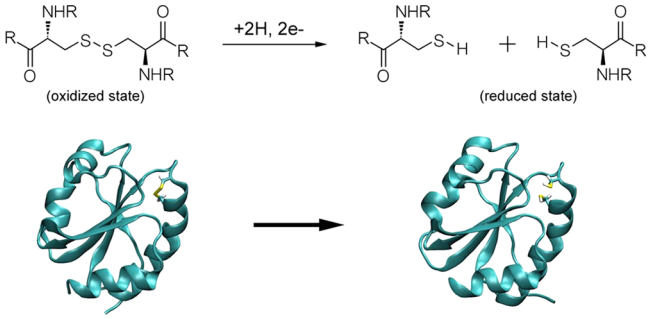

Figure 1. Cystine reduction. Top: Scheme of the reduction of cystine to two cysteines. Bottom: the reaction in Trx of *Staphylococcus aureus*.

opened during such a transformation. When a bond shall be opened, the bonded interactions (not only the bond itself but also the angles and dihedrals that enclose the bond) shall be transformed to nonbonded interactions. This represents a challenge in the setup of the free-energy calculations, as it requires the introduction of nonbonded interactions between atoms, which in the oxidized state were bonded, entailing an exclusion of any nonbonded term in this state.

Here, we constructed a hybrid cysteine/cystine force field on the basis of the CHARMM27 force field to enable the transformation between cystine and two free cysteines in the MD software GROMACS. This single topology approach was chosen as it can be expected to converge faster than a dual topology approach,[34,35] as it minimizes the number of dummy atoms and perturbed degrees of freedom.[36] We introduced a new cysteine residue type, which extends the disulfide bonded cysteine (CYS2) in the CHARMM27 force field by adding one atom HUD and two virtual sites (V_c and V_s). The dummy atom and virtual sites do not have bonded interactions and LJ interactions. The new residue was named CYD (Figure 2).

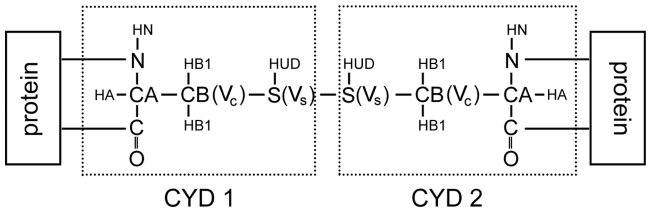

Figure 2. Scheme of the CYD topology. CYD corresponds to a disulfide-bonded cysteine residue but was expanded by one atom, HUD, that will be transformed into a hydrogen, and two virtual sites, V_c and V_s (shown in the brackets), that are constrained to the same positions as CB and S, respectively. Here, two CYD residues form a disulfide bond in a protein as shown schematically.

HUD with a mass of a hydrogen atom is bonded to the sulfur. The distance between V_c (V_s) and CA (CB) is constrained to be the same as the one between CB (S) and CA (CB). Thus, the virtual sites V_c and V_s colocalize with CB and S, respectively. The nonbonded interactions between V_c (V_s) and those atoms in CYD separated by no more than three bonds with CB (S) are excluded. At $\lambda = 0$, the dummy HUD and two virtual sites (V_c and V_s) have zero charge and thus have no interactions with any other atoms in the system. Therefore, CYD at $\lambda = 0$ corresponds exactly to CYS2.

Analogously, we want to reproduce the open cysteine state, CYS, in CHARMM27 with CYD at $\lambda = 1$. At $\lambda = 1$, HUD is transformed into a hydrogen atom and shows all bonded interactions of the hydrogen atom bonded to the sulfur in CYS, but several nonbonded interactions with HUD, as listed in Table 1, are missing. There are some bonded interactions

Table 1. Nonbonded Interactions Added to the Pair List To Enable CYD at $\lambda = 0$ and $\lambda = 1$ to Reproduce CYS2 and CYS, Respectively[a]

particle 1	particle 2	$\lambda = 0$	$\lambda = 1$
S_1	CA_2	1−4	short
S_2	CA_1	1−4	short
S_1[b]	$HB1_2$	1−4	short
S_2	$HB1_1$	1−4	short
CB_1[b]	CB_2	1−4	short
V_{s1}	CB_2	off	on
V_{s2}	CB_1	off	on
V_{s1}	S_2	off	on
HUD_1	CB_2	off	on
HUD_2	CB_1	off	on
HUD_1	S_2	off	on
HUD_2	S_1	off	on
HUD_1	HUD_2	off	on
V_c[c]	HN	off	off
V_s[c]	N	off	off
V_c[c]	O	off	off
V_s[c]	HA	off	off
V_s[c]	C	off	off

[a]GROMACS distinguishes nonbonded interactions between atoms separated by exactly three bonds, i.e., 1−4 interactions, and short-range interactions between atoms separated by more than three bonds. Here, "1−4" and "short" refer to the former and latter, respectively. [b]This applies to the two HB1s. [c]This applies to both CYDs. The subscripts 1 and 2 refer to atoms in CYD1 and CYD2, respectively.

present in cystine which ought to be absent in two independent cysteine residues, the most obvious being the bond S_1-S_2 and the angle $CB_1-S_1-S_2$. Here, the subscripts 1 and 2 refer to atoms in CYD1 and CYD2, respectively (compare in Figure 2). These bond and angle potentials can be switched to zero at $\lambda = 1$, but they will lead to an exclusion of some of the nonbonded interactions necessary to represent the two CYS. To circumvent this exclusion, V_c and V_s carry nonbonded interactions at $\lambda = 1$. In addition, some interactions, such as the LJ interaction between CA_1 and S_2, are 1−4 interactions at $\lambda = 0$ but short-range LJ interactions at $\lambda = 1$. The necessary transformation of all these nonbonded interactions are added to the pair list and are summarized in Table 1.

RESULTS AND DISCUSSION

We here used free-energy calculations (FEC) to estimate the redox potential of proteins that undergo thiol/disulfide exchange. To test the applicability of the method to a wide range of thiol−disulfide oxidoreductases, we chose thioredoxin (Trx), glutaredoxin (Grx1 and Grx3), and several thiol−disulfide oxidoreductases in disulfide bond formation systems (DsbA, DsbL, and DsbC) from *Escherichia coli*, whose redox potentials range from −270 mV to −95 mV (Table 2). In addition, to check whether the method will resolve the differences in redox potential caused by single-residue mutations, we chose Trx from *E. coli* and three Pro34 mutants, that is, P34A, P34D, and P34K, and Trx from *Staphylococcus aureus* and two Pro31 mutants (P31S and P31T, the *S. aureus* wild type and its mutants were missing residues 1−3, which is

DOI: 10.1021/acs.jpcb.5b01051
J. Phys. Chem. B 2015, 119, 5386−5391

Table 2. Experimental Redox Potentials and Starting Structures of the Tested Proteins

starting structure			
name	oxidized state	reduced state	redox potential (mV)
EC WT[a]	1XOA	1XOB	−270[37]
P34A[a]	[c]	[d]	−250[37]
P34D[a]	[c]	[d]	−254[37]
P34K[a]	[c]	[d]	−242[37]
SA WT[b]	2O7K	[d]	−268[38]
P31T[b]	2O85	[d]	−236[38]
P31S[b]	2O87	[d]	−244[38]
EcGrx1[a]	3C1R	[d]	−233[39]
EcGrx3[a]	1FOV	[d]	−198[39]
EcDsbC[a]	1EEJ (Chain A)	[d]	−140[6]
EcDsbA[a]	[d]	1A23	−122[6]
EcDsbL[a]	[d]	3C7M (Chain A)	−95[6]

[a]From *E. coli*. [b]From *S. aureus*. [c]Modeled from 1XOA. [d]Taking the end structure of the transformation from its oxidized or reduced counterpart.

why the mutations refer to the 31st residue instead of to the 34th residue). As shown in Table 2, the redox potentials for Trx and its mutants are quite close falling into a narrow range from −270 mV to −236 mV. All thiol−disulfide oxidoreductases tested share the *CXXC* motif common to all Trx-like proteins.

For most of the 12 proteins tested, either the oxidized or the reduced structures have been experimentally resolved. The structures of the *E. coli* Trx mutants (P34A, P34D, and P34K) were not available and were modeled from their oxidized wild type (pdb entry: 1XOA) using the Molecular Operating Environment software (MOE 2008.10; Chemical Computing Group, Quebec, Canada). For proteins with only the oxidized or reduced structure available, the reduced or oxidized counterpart was modeled on the basis of the available structure. The starting structures for all proteins are listed in Table 2. The hybrid cysteine/cystine force field was used to describe the transition between the oxidized and the reduced state.

To estimate the redox potential of each protein with CGI, 500 input structures were taken evenly from the last 10 ns of a longer equilibrium simulation of the oxidized and reduced state as described in the Computational Methods. For each input structure, an alchemical transformation was performed within 200 ps with initial velocities taken from a Maxwell−Boltzmann distribution. Transitions were simulated for a total of 100 ns for each protein, requiring ∼1 day of computing time on 100 CPUs. The forward (backward) work W_f (W_b) for the transformation from the oxidized (reduced) state to the reduced (oxidized) state was then obtained from integrating $\delta H_\lambda/\delta\lambda$ over the whole transformation (eq 3). The histograms of the forward and backward work are shown in Figure S1 of the Supporting Information. For all proteins, the distributions of forward and backward work overlapped very well. Thus, we are confident that nonequilibrium simulations can accurately estimate free-energy differences,[40,41] even for systems with significant conformational changes.[42]

The intersection point of the Gaussian-fitted forward and backward work distributions gave the free-energy difference ΔG and, using Nernst's equation (eq 1), the redox potential. Figure 3A compares the estimated redox potentials and the corresponding experimental values. We obtained a Pearson correlation coefficient of 0.72 for this very diverse set of 12 redox proteins and mutants. Spearman's rank correlation coefficient was estimated to be 0.61 with a p-value of 0.04. Both statistical results are satisfying and imply that our method is able to correctly rank the redox potentials of different thiol/

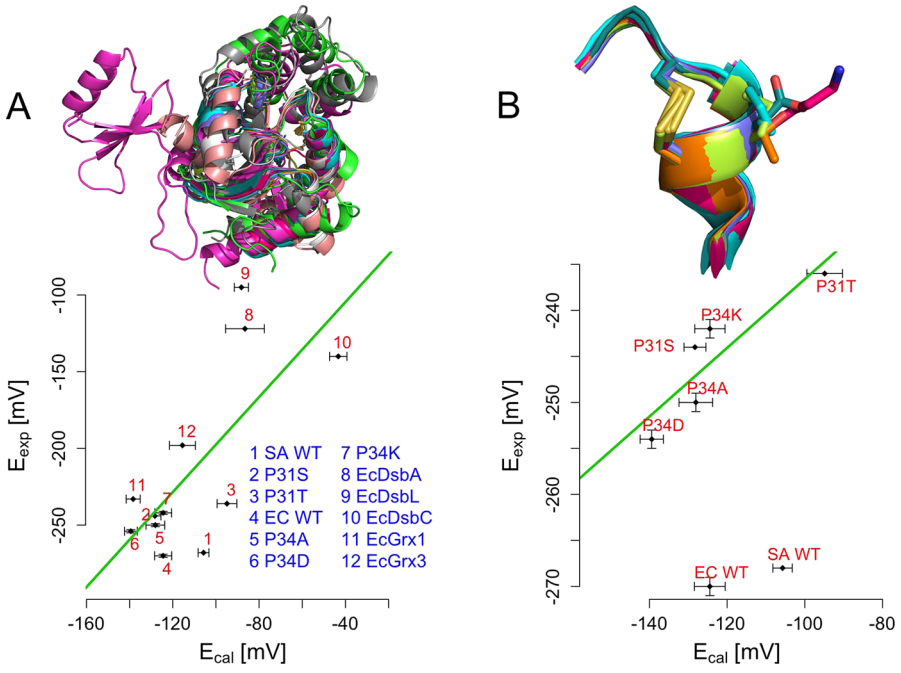

Figure 3. Comparison of the calculated and experimental redox potentials of tested proteins. (A) Redox potentials for all 12 proteins of the thioredoxin superfamily, all of which are shown on the top in cartoon representation after least-squares fitting. (B) Redox potentials of Trx only. A zoom onto the *CXXC* motif, with the catalytic cysteine and the mutated residue highlighted as sticks, is shown on the top. The green line is a linear fit. Redox potentials of wild-type proteins of Trx in B were overestimated, and a likely explanation is that their higher pK_a compared to the mutants. The standard deviation of the calculated redox potential is estimated using eq 8 in ref 22.

DOI: 10.1021/acs.jpcb.5b01051
J. Phys. Chem. B 2015, 119, 5386−5391

disulfide exchange proteins, given they vary by ∼50 mV or more. A linear fit gives the following relationship between them with a residual error of 42 mV (8.1 kJ/mol): $E_{exp} = 1.5 \cdot E_{cal} - 43$ mV. A constant shift in redox potential, here by 43 mV, can be expected, since the free-energy calculations neglect the free-energy contribution from removing two protons and two electrons from the system. The slope of 1.5 indicates that our method underestimates differences in redox potential among the protein test set, which might be due to inaccuracies in the protein and water force field used. This trend could be force field but also system dependent.

We next analyzed the predictive power of the CGI method for redox potential changes upon mutation. The seven experimentally determined Trx wild-type and mutant redox potentials vary by only up to ∼35 mV. Nevertheless, we here were able to correctly rank all five mutants of the data set in terms of their redox potential. The wild-type proteins, carrying a CXPC motif, however, fall out of this trend and were predicted to have a too high redox potential. One possible reason for the disagreement between experiment and our calculations is that wild-type Trx's have been observed to show a higher pK_a for the catalytic cysteines.[38] We indeed obtained a higher pK_a for SA Trx and Ecoli Trx by 0.5 and 1, respectively (Table S1 of the Supporting Information), which at least partly can account for the overestimation of their redox potential. Leaving out the proline-containing wild-type Trx's from the fit, we obtained a Pearson correlation coefficient of 0.89 (see Figure 3B). The prediction error is 3.2 mV (0.6 kJ/mol). In addition, Spearman's rank correlation coefficient was improved to be 0.9 with a p-value of 0.08. The greatly improved accuracy is probably due to the mutants experiencing a similar chemical environment and compares well to the previously reported error of ∼4 kJ/mol obtained for the metal center of a flavoprotein and its mutants.[20] Different proteins such as Dsb and Grx proteins, even though from the same family, feature a drastically modified chemical environment around the disulfide bond or thiols of interest, resulting in higher differences in measured redox potentials and similarly in larger uncertainties in the prediction.

CONCLUSIONS

Differences in redox potential of proteins are the driving force of many vital biochemical reactions. A fundamental understanding of redox processes under physiological conditions opens up opportunities to get deeper insights into biochemical pathways. While redox potentials of proteins are in principle experimentally accessible, an alternative computational approach would allow to systematically screen and tune redox properties of proteins by mutagenesis, prior to the more elaborate experimental validation.

We here calculated redox potentials of thiol/disulfide pairs from MD simulations through the CGI Method. A hybrid cysteine/cystine force field was constructed to enable the calculation of the change in free energy upon disulfide bond reduction. The predicted redox potentials of a total of 12 proteins are in good quantitative agreement with the experimental values, with an overall correlation coefficient of 0.72. The method is also able to quantify the redox potential difference due to a single-point mutation in thioredoxins. Therefore, the approach paves the way toward a rational design of protein mutants with tailored redox potentials. We expect further improvements of the method by allowing polarization of the thiol/disulfide bond in response to their electrostatic environment as observed for metalloproteins,[43] by considering dynamic changes in protonation states in the redox system[44] or by testing other force fields.

Taken together, our approach can be used to study disulfide bond stability in terms of their redox potential in diverse chemical surroundings, including the interesting case of allosteric disulfide bonds.[45] Expanding the thermodynamic cycle and perturbing different types of interactions (e.g., electrostatic versus Lennard-Jones) after each other might allow the dissection of the contributions determining a disulfide's redox potential, such as internal strain,[46,47] electrostatic (de)stabilization, or steric effects. It may provide a guidance to introduce disulfide bonds into proteins devoid of any disulfide bond[48] or to rationally tune a disulfide bond's redox potential by protein engineering. Furthermore, the concept of a hybrid topology together with the CGI method can be extended to the free-energy calculation of other bond-breaking reactions with molecular mechanics, such as the mutation of proline to another amino acid, and thus can widen the range of applications of free-energy calculations.

ASSOCIATED CONTENT

Supporting Information

Results of pK_a calculations and work distributions in FEC are given. This material is available free of charge via the Internet at http://pubs.acs.org/.

AUTHOR INFORMATION

Corresponding Author

*E-mail: frauke.graeter@h-its.org.

Present Address

‡(W.L.) Bioengineering Department, University of Illinois at Chicago.

Author Contributions

§(W.L., I.B.B.) These authors contributed equally.

Notes

The authors declare no competing financial interest.

ACKNOWLEDGMENTS

The authors thank Sang Paik for carefully reading the manuscript, Tobias Dick and members of the Molecular Biomechanics group for fruitful discussions, and the Klaus Tschira Foundation and the Deutsche Forschungsgemeinschaft (Sachbeihilfe GR3494/2-2) for financial support.

REFERENCES

(1) Banerjee, R.; Becker, D.; Dickman, M.; Gladyshev, V.; Ragsdale, S. *Redox Biochemistry*; John Wiley & Sons, Inc.: Hoboken, NJ, 2008.

(2) Nagahara, N. Intermolecular Disulfide Bond To Modulate Protein function as a Redox-sensing Switch. *Amino Acids* **2011**, *41*, 59−72.

(3) Fass, D. Disulfide Bonding in Protein Biophysics. *Annu. Rev. Biophys.* **2012**, *41*, 63−79.

(4) Jacob, C.; Winyard, P. G. *Redox Signaling and Regulation in Biology and Medicine*; Wiley-VCH Verlag GmbH & Co. KGaA: Weinheim, Germany, 2009.

(5) Wouters, M. A.; Fan, S. W.; Haworth, N. L. Disulfides as Redox Switches: From Molecular Mechanisms to Functional Significance. *Antioxid. Redox Signaling* **2010**, *12*, 53−91.

(6) Ito, K.; Inaba, K. The Disulfide Bond Formation (Dsb) System. *Curr. Opin. Struct. Biol.* **2008**, *18*, 450−458.

DOI: 10.1021/acs.jpcb.5b01051
J. Phys. Chem. B 2015, 119, 5386−5391

(7) Arnér, E. S.; Holmgren, A. Physiological Functions of Thioredoxin and Thioredoxin Reductase. *Eur. J. Biochem.* **2000**, *267*, 6102−6109.
(8) Fernandes, A. P.; Holmgren, A. Glutaredoxins: Glutathione-dependent Redox Enzymes with Functions Far Beyond a Simple Thioredoxin Backup System. *Antioxid. Redox Signaling* **2004**, *6*, 63−74.
(9) Quan, S.; Schneider, I.; Pan, J.; Von Hacht, A.; Bardwell, J. C. The CXXC Motif Is More Than a Redox Rheostat. *J. Biol. Chem.* **2007**, *282*, 28823−28833.
(10) Lin, T.-Y. Protein-protein Interaction as a Powering Source of Oxidoreductive Reactivity. *Mol. Biosyst.* **2010**, *6*, 1454−1462.
(11) Huber-Wunderlich, M.; Glockshuber, R. A Single Dipeptide Sequence Modulates the Redox Properties of a Whole Enzyme Family. *Folding Des.* **1998**, *3*, 161−171.
(12) Lin, T. Y.; Kim, P. S. Urea Dependence of Thiol-disulfide Equilibria in Thioredoxin: Confirmation of the Linkage Relationship and a Sensitive Assay for Structure. *Biochemistry* **1989**, *28*, 5282−5287.
(13) Blumberger, J.; Bernasconi, L.; Tavernelli, I.; Vuilleumier, R.; Sprik, M. Electronic Structure and Solvation of Copper and Silver Ions: A Theoretical Picture of a Model Aqueous Redox Reaction. *J. Am. Chem. Soc.* **2004**, *126*, 3928−3938.
(14) van den Bosch, M.; Swart, M.; Berendsen, H. J.; Mark, A. E.; Oostenbrink, C.; van Gunsteren, W. F.; Canters, G. W. Calculation of the Redox Potential of the Protein Azurin and Some Mutants. *ChemBioChem.* **2005**, *6*, 738−746.
(15) Hughes, T. F.; Friesner, R. A. Development of Accurate DFT Methods for Computing Redox Potentials of Transition Metal Complexes: Results for Model Complexes and Application to Cytochrome P450. *J. Chem. Theory Comput.* **2012**, *8*, 442−459.
(16) Blumberger, J. Free Energies for Biological Electron Transfer from QM/MM Calculation: Method, Application and Critical Assessment. *Phys. Chem. Chem. Phys.* **2008**, *10*, 5651−5667.
(17) Zeng, X.; Hu, H.; Hu, X.; Yang, W. Calculating Solution Redox Free Energies with Ab Initio Quantum Mechanical/Molecular Mechanical Minimum Free Energy Path Method. *J. Chem. Phys.* **2009**, *130*, 164111/1−164111/8.
(18) Baldus, I.; Gräter, F. Mechanical Force Can Fine-tune Redox Potentials of Disulfide Bonds. *Biophys. J.* **2012**, *102*, 622−629.
(19) Kamerlin, S. C.; Haranczyk, M.; Warshel, A. Progress in Ab Initio QM/MM Free-Energy Simulations of Electrostatic Energies in Proteins: Accelerated QM/MM Studies of pKa, Redox Reactions and Solvation Free Energies? *J. Phys. Chem. B* **2009**, *113*, 1253−1272.
(20) Sattelle, B. M.; Sutcliffe, M. J. Calculating Chemically Accurate Redox Potentials for Engineered Flavoproteins from Classical Molecular Dynamics Free Energy Simulations? *J. Phys. Chem. A* **2008**, *112*, 13053−13057.
(21) Filippini, G.; Goujon, F.; Bonal, C.; Malfreyt, P. Toward a Prediction of the Redox Properties of Electroactive SAMs: A Free Energy Calculation by Molecular Simulation. *J. Phys. Chem. B* **2010**, *114*, 12897−12907.
(22) Goette, M.; Grubmüller, H. Accuracy and Convergence of Free Energy Differences Calculated from Nonequilibrium Switching Processes. *J. Comput. Chem.* **2009**, *30*, 447−456.
(23) Crooks, G. E. Nonequilibrium Measurements of Free Energy Differences for Microscopically Reversible Markovian Systems. *J. Stat. Phys.* **1998**, *90*, 1481−1487.
(24) Crooks, G. E. Entropy Production Fluctuation Theorem and the Nonequilibrium Work Relation for Free Energy Differences. *Phys. Rev. E* **1999**, *60*, 2721.
(25) Hess, B.; Kutzner, C.; van der Spoel, D.; Lindahl, E. GROMACS 4: Algorithms for Highly Efficient, Load-balanced, and Scalable Molecular Simulation. *J. Chem. Theory Comput.* **2008**, *4*, 435−447.
(26) Jorgensen, W. L.; Chandrasekhar, J.; Madura, J. D.; Impey, R. W.; Klein, M. L. Comparison of Simple Potential Functions for Simulating Liquid Water. *J. Chem. Phys.* **1983**, *79*, 926−935.
(27) Bussi, G.; Donadio, D.; Parrinello, M. Canonical Sampling Through Velocity Rescaling. *J. Chem. Phys.* **2007**, *126*, 014101/1−014101/7.
(28) Hess, B. P.-LINCS: A Parallel Linear Constraint Solver for Molecular Simulation. *J. Chem. Theory Comput.* **2008**, *4*, 116−122.
(29) Essmann, U.; Perera, L.; Berkowitz, M. L.; Darden, T.; Lee, H.; Pedersen, L. G. A Smooth Particle Mesh Ewald Method. *J. Chem. Phys.* **1995**, *103*, 8577−8593.
(30) Nilges, M.; Clore, G. M.; Gronenborn, A. M. Determination of Three-dimensional Structures of Proteins from Interproton Distance Data by Dynamical Simulated Annealing from a Random Array of Atoms Circumventing Problems Associated with Folding. *FEBS Lett.* **1988**, *239*, 129−136.
(31) Beutler, T. C.; Mark, A. E.; van Schaik, R. C.; Gerber, P. R.; van Gunsteren, W. F. Avoiding Singularities and Numerical Instabilities in Free Energy Calculations Based on Molecular Simulations. *Chem. Phys. Lett.* **1994**, *222*, 529−539.
(32) Schäfer, H.; Van Gunsteren, W. F.; Mark, A. E. Estimating Relative Free Energies from a Single Ensemble: Hydration Free Energies. *J. Comput. Chem.* **1999**, *20*, 1604−1617.
(33) Gapsys, V.; Seeliger, D.; de Groot, B. L. New Soft-core Potential Function for Molecular Dynamics Based Alchemical Free Energy Calculations. *J. Chem. Theory Comput.* **2012**, *8*, 2373−2382.
(34) Gao, J.; Kuczera, K.; Tidor, B.; Karplus, M. Hidden Thermodynamics of Mutant Proteins: A Molecular Dynamics Analysis. *Science* **1989**, *244*, 1069−1072.
(35) Axelsen, P. H.; Li, D. Improved Convergence in Dual-topology Free Energy Calculations through Use of Harmonic Restraints. *J. Comput. Chem.* **1998**, *19*, 1278−1283.
(36) Pearlman, D. A. A Comparison of Alternative Approaches to Free Energy Calculations. *J. Phys. Chem.* **1994**, *98*, 1487−1493.
(37) Jeng, M.-F.; Campbell, A. P.; Begley, T.; Holmgren, A.; Case, D. A.; Wright, P. E.; Dyson, H. J. High-resolution Solution Structures of Oxidized and Reduced *Escherichia coli* Thioredoxin. *Structure* **1994**, *2*, 853−868.
(38) Roos, G.; Garcia-Pino, A.; Brosens, E.; Wahni, K.; Vandenbussche, G.; Wyns, L.; Loris, R.; Messens, J. The Conserved Active Site Proline Determines the Reducing Power of *Staphylococcus aureus* Thioredoxin. *J. Mol. Biol.* **2007**, *368*, 800−811.
(39) Åslund, F.; Berndt, K. D.; Holmgren, A. Redox Potentials of Glutaredoxins and Other Thiol-disulfide Oxidoreductases of the Thioredoxin Superfamily Determined by Direct Protein-protein Redox Equilibria. *J. Biol. Chem.* **1997**, *272*, 30780−30786.
(40) Pohorille, A.; Jarzynski, C.; Chipot, C. Good Practices in Free-energy Calculations. *J. Phys. Chem. B* **2010**, *114*, 10235−10253.
(41) Dellago, C.; Hummer, G. Computing Equilibrium Free Energies Using Non-equilibrium Molecular Dynamics. *Entropy* **2013**, *16*, 41−61.
(42) Park, S.; Khalili-Araghi, F.; Tajkhorshid, E.; Schulten, K. Free Energy Calculation from Steered Molecular Dynamics Simulations Using Jarzynskis Equality. *J. Chem. Phys.* **2003**, *119*, 3559−3566.
(43) Wei, C.; Lazim, R.; Zhang, D. Importance of Polarization Effect in the Study of Metalloproteins: Application of Polarized Protein Specific Charge Scheme in Predicting the Reduction Potential of Azurin. *Proteins: Struct., Funct., Bioinf.* **2014**, *82*, 2209−2219.
(44) Donnini, S.; Tegeler, F.; Groenhof, G.; Grubmueller, H. Constant pH Molecular Dynamics in Explicit Solvent with λ-dynamics. *J. Chem. Theory Comput.* **2011**, *7*, 1962−1978.
(45) Schmidt, B.; Ho, L.; Hogg, P. J. Allosteric Disulfide Bonds. *Biochemistry* **2006**, *45*, 7429−7433.
(46) Zhou, B.; Baldus, I. B.; Li, W.; Edwards, S. A.; Gräter, F. Identification of Allosteric Disulfides from Prestress Analysis. *Biophys. J.* **2014**, *107*, 672−681.
(47) Kucharski, T. J.; Huang, Z.; Yang, Q.-Z.; Tian, Y.; Rubin, N. C.; Concepcion, C. D.; Boulatov, R. Kinetics of Thiol/disulfide Exchange Correlate Weakly with the Restoring Force in the Disulfide Moiety. *Angew. Chem., Int. Ed.* **2009**, *48*, 7040−7043.
(48) Matsumura, M.; Matthews, B. W. Control of Enzyme Activity by an Engineered Disulfide Bond. *Science* **1989**, *243*, 792−794.

DOI: 10.1021/acs.jpcb.5b01051
J. Phys. Chem. B 2015, 119, 5386−5391